JOURNAL OF NEUROPHYSIOLOGY
Vol. 39, No. 4, July 1976. *Printed in U.S.A.*

Modulation of Spike Frequency by Regions of Special Axonal Geometry and by Synaptic Inputs

M. E. SPIRA, Y. YAROM, AND I. PARNAS
Neurobiology Unit, Hebrew University, Jerusalem, Israel

SUMMARY AND CONCLUSIONS

1. Spike propagation across the nonhomogeneous section of the giant axon in ganglion T_3 of the cockroach was analyzed by intracellular microelectrodes recording at the posterior and anterior ends of T_3. Ascending and descending potentials were evoked by stimulation of A_5–A_6 and T_2–T_3 connectives.

2. At high frequencies, descending and ascending impulses exhibit the following: *a*) consecutive reduction in the spike amplitude, *b*) a decrease in the afterhyperpolarization; *c*) gradual appearance of a prepotential together with an increase in delay of spike initiation; *d*) failure of full spike invasion into the recording area, showing only a decremental potential.

3. The duration of a train required to block spike propagation when the whole connective is stimulated is much shorter (about 6 times) than that required when a single giant axon is stimulated.

4. The conduction block is associated with a marked decrease in effective membrane resistance, greater than that expected from depolarization and delayed rectification.

5. Synaptic potentials could be recorded in the giant axons in the caudal base of ganglion T_3 after stimulation of either the ipsilateral or contralateral connectives at both ends of the ganglion. These synaptic potentials could be blocked by *d*-tubocurarine (*d*-TC) or low Ca^{2+}-high Mg^{2+}.

6. Activation of these synapses produces a marked increase in membrane conductance, blocking propagation of spike trains through the ganglion.

7. After these synapses are blocked by *d*-TC or low Ca^{2+}-high Mg^{2+}, high-frequency stimulation still produces a conduction block.

8. It seems that conduction of spike during repetitive stimulation is affected both by accumulation of extracellular potassium, which depolarizes the membrane and causes sodium inactivation, and by activation of synaptic inputs to shunt the membrane in this region.

8. Each of these two mechanisms by itself can produce conduction block along the giant axons in ganglion T_3.

INTRODUCTION

Contrary to the classical concept, axons do not always transmit their pattern of conducted impulses accurately to each of their main and terminal branches (6, 12, 18, 23, 40–43). Changes in spike pattern occur in regions of special geometry such as at branch points and points of sudden change in axon diameter. Furthermore, the channeling of different information into different branches or sections of a single axon depends on the past history of the axon's activity (38).

In most of the experimental systems where such changes in spike pattern or conduction block have been demonstrated it is difficult to study the underlying mechanisms, mainly because intracellular recordings cannot be made from the points of interest (6, 40). Most of the conclusions as to mechanisms have, therefore, been drawn either from extracellular recordings (6, 23) or from intracellular recordings made at the soma and, thus, reflecting events occurring in a remote region (40, 41).

The giant axons of the cockroach (28) and the bifurcating axon of the lobster (23), on the other hand, offer convenient models for studying dynamic changes that occur in special regions during repetitive firing. The giant axons of the cockroach are continuous through the length of the nervous system (10, 36, 37) and emit several branches while passing through the metathoracic ganglion (5, 10, 13, 31, 35). These axons can transmit single-action potentials in both directions past the ganglion. At 50 Hz, however, anteroposterior (descending) conduction is rapidly blocked, while posteroanterior (ascending) conduction persists for much longer periods (28). Similarly, Grossman, Spira, and Parnas (12) succeeded in recording intracellu-

Received for publication August 18, 1975.

larly from an isolated bifurcating axon of the lobster and demonstrated that at high frequencies of stimulation, conduction was blocked along one branch while it persisted in the second.

This is the first of a series of articles in which we analyze some of the mechanisms involved in such conduction blocks using the cockroach giant axon system. The present article describes the events that take place during the development of a block. We show that the block is associated with an increase in membrane conductance, combined with a membrane depolarization produced mainly by the accumulation of potassium ions in the extracellular space. Thus, the region of the giant axons in ganglion T_3 with its special geometry is a zone of a low safety factor for spike conduction and is, therefore, the first to be blocked. In addition, we demonstrate the presence of synaptic inputs into the giant axon in ganglion T_3 and their ability to modulate the blocking frequency and, more importantly, to modulate the pattern of a train of spikes traversing the giant axons in either direction. The second article (5) is an ultrastructural study of the giant axons in ganglion T_3, showing that these axons emit branches in ganglion T_3 and that these branches receive synaptic inputs. The third paper (26) is a theoretical analysis which, using the Hodgkin Huxley equations (15) modified for the conduction of action potentials in an inhomogeneous axon, simulates the development of the frequency block and predicts some of its consequences.

METHODS

Preparation

Adult males of the cockroach *Periplaneta americana* were used. The whole ventral nerve cord was isolated as previously described (36). It was then pinned ventral side up in a Sylgard chamber for easier access to the ventral giant axons.

Recording and stimulation

A diagram of the experimental system is given in Fig. 1. The T_2–T_3 and A_5–A_6 connectives were stimulated with silver-chloride hook electrodes (St_1, St_2 in Fig. 1). Intracellular recordings were made with glass microelectrodes filled with 3 M KCl (10–15 MΩ resistance) using conventional electrophysiological techniques. Intracellular recordings were made both at the posterior and anterior ends of the metathoracic ganglion (R_1, R_2 in Fig. 1). The criteria for deciding that the microelectrodes were indeed in an abdominal giant axon were: *a*) action potentials could be evoked by stimulating the A_5–A_6 and the T_2–T_3 connectives and could be collided by stimulating both (bidirectional conduction (36)), and *b*) the minimal value of conduction velocity of action potentials induced at A_5–A_6 had to be between 4 and 5 m/s (34). For the determination of effective membrane resistance two microelectrodes were inserted into a giant axon on both sides of ganglion T_3. Ramp current pulses were injected through the anterior microelectrode and the resulting membrane potential drop was measured by the posterior electrode.

Solutions

The bathing solution used was that given by Kerkut et al. (20) and was composed of NaCl 214 mM, KCl 3.1 mM, $CaCl_2$ 9 mM, and Tris 1 mM. The pH was adjusted to 7.2–7.3. In "calcium-free" solutions, the calcium was replaced by 9 mM $MgCl_2$. Bath temperature was 20–23°C.

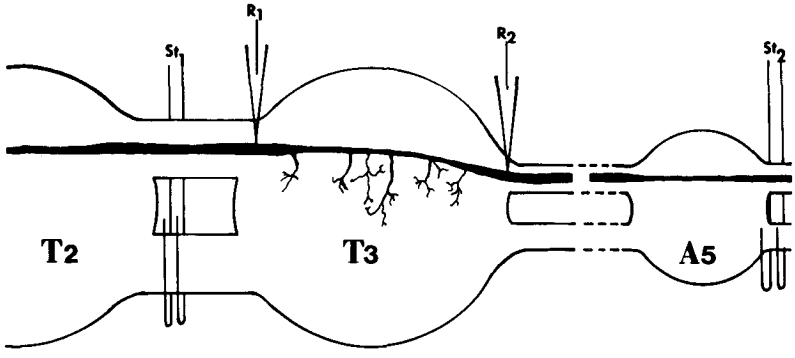

FIG. 1. Diagrammatic representation of the experimental setup. T_2, T_3: mesothoracic and metathoracic ganglia. A_5: fifth abdominal ganglion. St_1, St_2: silver chloride stimulating electrodes. R_1, R_2: intracellular microelectrodes. The giant axon is not drawn to scale. Note the slight narrowing of the axon within ganglion T_3 and the presence of axonal branches.

RESULTS

Block of conduction at high frequency: descending impulses

A giant axon was impaled at the posterior base of ganglion T_3 and the connectives were stimulated at T_2–T_3. In general, during stimulation at high frequency, the following changes were observed: *1*) consecutive reduction in spike amplitude, *2*) a decrease in the size of the afterhyperpolarization, *3*) gradual appearance of a prepotential together with an increase in the delay of spike initiation, *4*) intermittent failure of spike invasion into the recording area and the consequent observation of only a decremental potential. These changes were superimposed on a membrane depolarization sometimes reaching values of 20 mV at a high stimulation frequency (100 Hz).

Figure 2 summarizes results of two such experiments (Fig. 2*A–D* from one experiment, and *E–H* from another experiment). When the T_2–T_3 connectives were stimulated at a low frequency (1 Hz), even for long periods (30 min), action potentials of a constant amplitude and delay were recorded at the posterior base of ganglion T_3 (Fig. 2*A*; *E*, lower traces). Following an increase of stimulus frequency to 33 Hz, the spike amplitude initially decreased and a prepotential appeared (Fig. 2*B*). During this period the membrane potential was depolarized by about 7 mV (not obvious in Fig. 2 but see Fig. 4*A*). The delay to the peak of the spike became not constant and the spike amplitude became further reduced (Fig. 2*C*). After 128 s of stimulation there was a complete block of spike invasion and only a potential of 20 mV was recorded (not shown). With further stimulation this potential was reduced to 17 mV (Fig. 2*D*). As already described by Parnas et al. (28), this small potential is decremental, originating from a spike whose invasion into the recording area is blocked.

In Fig. 2*E–H* we demonstrate results from a similar experiment recorded at a higher gain (Figs. 2*E–H*, upper beams) to demonstrate the changes in the afterhyperpolarization. At a low frequency of 1 Hz, marked afterhyperpolarization was observed (Fig. 2*E*). During repetitive stimulation at 50 Hz, the afterhyperpolarization

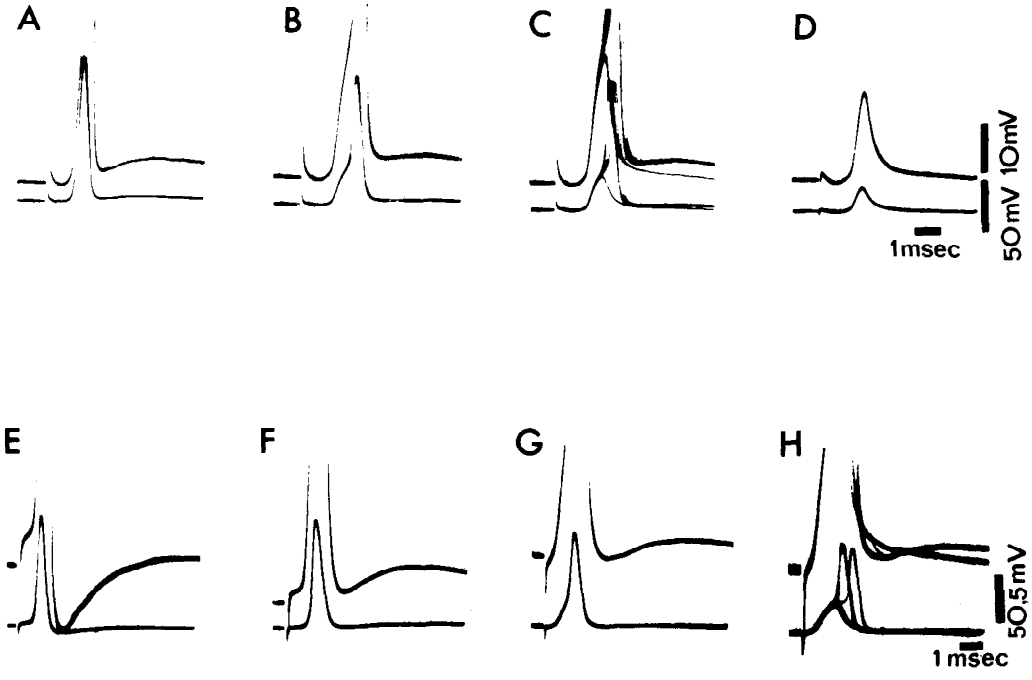

FIG. 2. Effects of high-frequency stimulation on descending spikes, recorded at the posterior base of ganglion T_3 (position R_2) following stimulation at T_2–T_3. The two sweeps show the same events at low and high gains. *A–D*: stimulation at 33/s (superimposed sweeps); *A*: during the 1st s of stimulation; *B*: after 78 s of continuous stimulation; *C*: after 82 s; *D*: after 147 s. Note that spike invasion is blocked intermittently in *C* and completely in *D* such that only a decremental potential of 17 mV is seen. For further detail see text. *E–H*: recordings at higher gain (upper sweeps) to demonstrate changes in afterhyperpolarization. Stimulation rate was 50/s. *E*: response after 1 s of stimulation; *F*: after 24 s; *G*: after 42 s; *H*: after 50 s of stimulation. In the lower sweep in *H* note the development of a prepotential.

was reduced (Fig. 2*F*, *G*) and when failure of invasion occurred, the afterhyperpolarization was absent altogether (Fig. 2*H*).

After cessation of stimulation and a period of rest, action potentials could be recorded again at the posterior base of ganglion T_3. The sequence of events during the recovery period was in the reversed order of that occurring during the development of the block. Invasion of single spikes into the recording area could be observed as early as 3–5 s after switching the stimulus rate to the low frequency (1 Hz). However, if now the axon was stimulated again at high frequency, conduction block developed after a few impulses. Only after the axon was allowed a long period of rest (20 min) could it sustain high-frequency activation as in the first experiment.

Effect of frequency of stimulation on rate of development of conduction block

In general the block developed much faster at higher frequencies. Figure 3 represents graphically the values of spike amplitude as it changed with time under different conditions of stimulation frequency. It can be seen that the complete conduction block was preceded by a period of intermittent conduction. After conduction block had developed, the remaining decremental potential was smaller for the higher stimulation frequencies.

Another parameter that varied with the frequency of stimulation was the membrane potential. Figure 4*A* shows the relation between the maximal change in the resting potential and the frequency of stimulation. It can be seen that the membrane depolarization was substantial, reaching 20 mV at 100 Hz. The rate of development of the depolarization with time also varied with the frequency, being faster at the higher frequencies (Fig. 4*B*).

Block of conduction at high frequency: ascending impulses

For these experiments a giant axon was impaled at the anterior base of ganglion T_3 and the connectives were stimulated at A_4–A_5 (see Fig. 1). Essentially the same sequence of events as described for the descending impulses took place. However, either the frequency or the duration of stimulation had to be greater in order to block conduction in the ascending direction.

In a few experiments, two microelectrodes were inserted into the same giant axon so that the events taking place during block in both ascending and descending directions could be recorded at the same time. In such an experiment at 50 Hz (Fig. 5), the invasion of descending impulses to the posterior base of T_3 was blocked after 25 s (Fig. 5*A*, *D*), and of ascending impulses into the anterior base of ganglion T_3 only after 40 s (Fig. 5*E*, *F*).

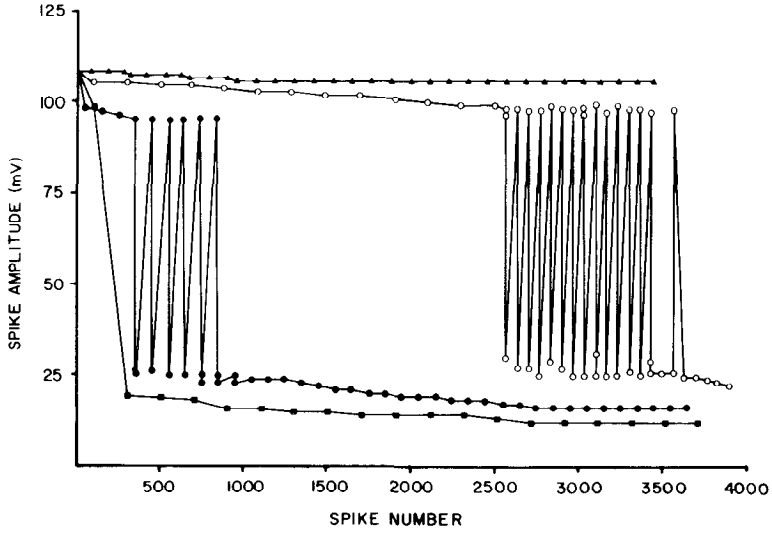

FIG. 3. Graphic representation of changes in spike amplitude during repetitive stimulation at different stimulation frequencies as a function of spike number in the train. The axon was stimulated continuously, and every second the camera shutter was opened for 100 ms. The spike number was computed from the duration of stimulation. Each point represents the range of amplitudes of the superimposed spikes. At places where more than one point appears, the spike amplitudes were such that they could be divided into discernible groups. Stimulation frequencies were: triangles, 25/s; open circle, 33/s; filled circles, 50/s; squares, 100/s. Note the change in the amplitude of the decremental potential after spike conduction has been blocked.

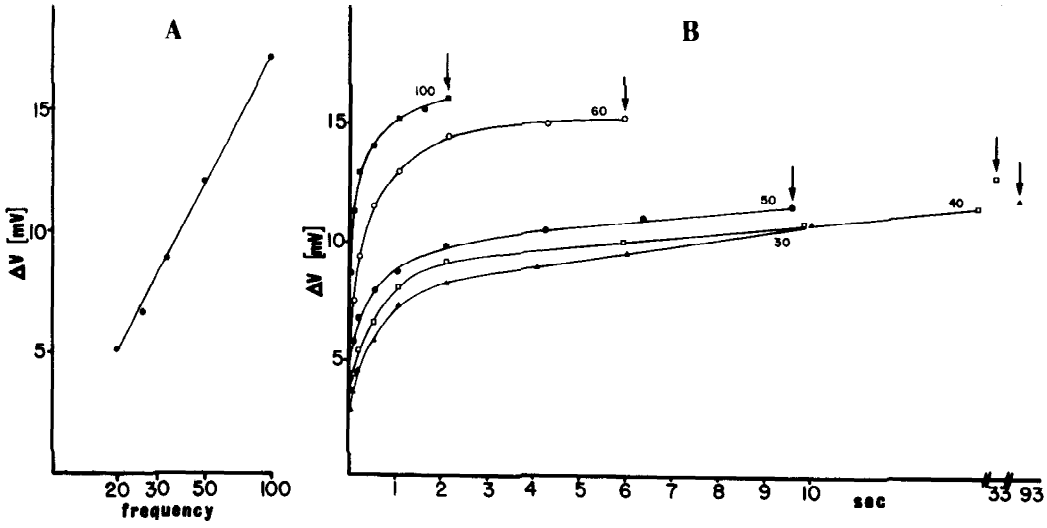

FIG. 4. *A*: semilog plot of the maximal depolarization as a function of stimulation frequency. *B*: depolarization as a function of time after the onset of stimulation at different stimulation frequencies. Arrows indicating time of block. Numbers represent stimulation frequency (Hz).

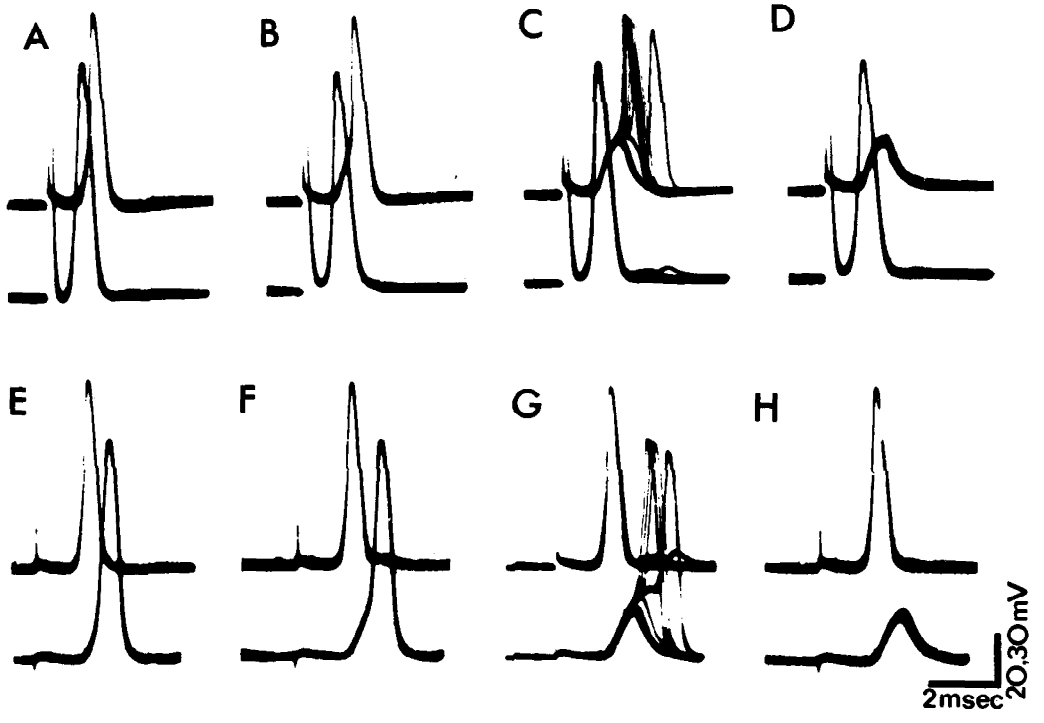

FIG. 5. Simultaneous recording of action potentials from a giant axon on both sides of ganglion T_3 during high-frequency stimulation. The upper and lower traces show responses recorded at the caudal and rostral bases of ganglion T_3, respectively. *A–D*: stimulation at T_2–T_3 (descending impulses) at 50/s. Note on continued stimulation the development of a prepotential at the posterior base and the appearance of a spike reflection at the anterior base (*C*). *E–H*: stimulation at A_4–A_5 (ascending impulses).

The findings that the conduction block in the ascending and descending directions is associated with both depolarization (Fig. 4) and reduction in the size of the afterhyperpolarization (Fig. 2 *E–H*) indicate an increase in extracellular potassium concentrations (11), obviously from the high-frequency activation of the axon. If the main factor in the development of the block is indeed extracellular potassium accumulation, then the conduction block that develops after stimulation at high frequency should not depend on the direction of propagation of the impulses producing the block. That is, the block produced by activation of the fiber in one direction (for example in the ascending direction) should also block conduction in the other direction (descending), and vice versa.

Figure 6 demonstrates a case where stimulation of the connective at A_4–A_5 (ascending impulses) at 100 Hz produced conduction block of a single test impulse evoked at T_2–T_3 (descending impulse).

Appearance of a reflection potential during high-frequency stimulation

When intracellular recordings were made at a point very close to ganglion T_3, an additional change in the shape of the spike was observed. This change is demonstrated in Fig. 5. During high-frequency stimulation, the spike recorded at the anterior wide region shows a prepotential (Fig. 5*C*, upper sweep) and a small potential is seen at the other end of the ganglion (Fig. 5*C*, lower sweep). The same phenomenon is observed for conduction in the opposite direction (Fig. 5*G*). It is clear from Fig. 5*C* and *G* that the small potential is a reflection of the delayed spike from the other side of the ganglion. A failure of invasion of the action potential into the wide region is associated with disappearance of the reflection potential (Fig. 5*D* and *H*).

Figure 6 shows another example of appearance of a reflection potential on the falling phase of the ascending spike recorded at the posterior base of ganglion T_3. The separation of the reflection potential from the falling phase of the spike (Fig. 6*C*, *D*) correlates with the development of a prepotential before the spike at the anterior end of the ganglion. The abrupt disappearance of this small potential (Fig. 6*D*, *E*, which occurred without the concomitant failure of the main ascending spike), indicates failure of invasion of the spike into the anterior wide region of the axon. Such spike reflec-

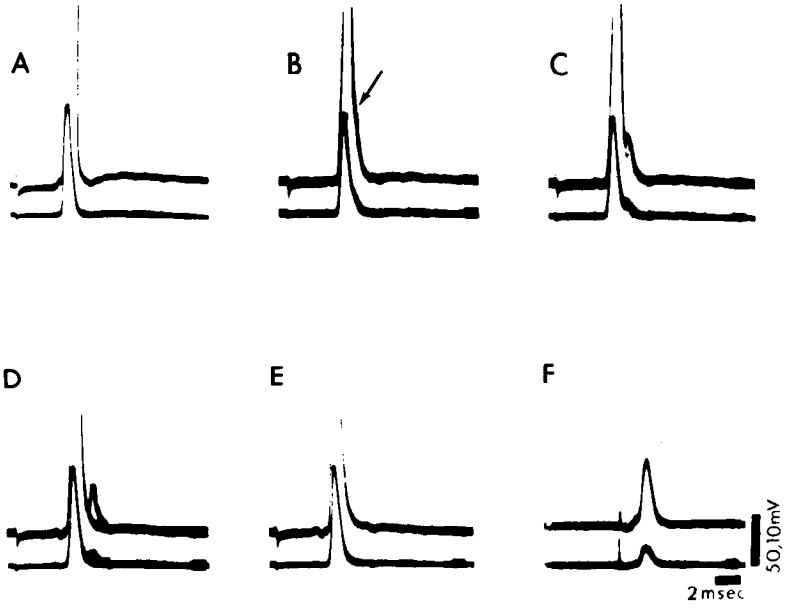

FIG. 6. Effects of high-frequency ascending impulses on the conduction of single descending impulses. Recordings were made at the posterior base of ganglion T_3 on stimulation at A_4–A_5 (ascending impulses) at 100/s. Lower and upper beams are at low and high gain, respectively. *A*: after 1 s of stimulation; *B*: after 11 s; *C*: after 13 s; *D*: after 17 s; *E*: after 20 s; *F*: response to a single test stimulus given at T_2–T_3 (descending impulse) immediately after *E*. Note that this single impulse is blocked and only a decremental potential is observed. From *B* to *D* the development and separation of a reflection potential (arrow) is observed. In *E* the reflection potential is absent because invasion of the ascending impulse into the anterior part of the ganglion is blocked (see text).

tions have been observed in regions of special geometry by Coombs, Curtis, and Eccles (7), Waxman, Pappas, and Bennett (44), and are predicted theoretically (21, 26, 33).

Effect of hyperpolarizing current on conduction at low and high frequency

As stated, the frequency block is associated with marked membrane depolarization probably due to the accumulation of extracellular potassium.

If indeed membrane depolarization is one of the major factors causing conduction block, then hyperpolarization of the membrane should restore conduction during high-frequency stimulation. The experiment illustrated in Fig. 7 confirms this prediction. Conduction of descending impulses was blocked after stimulating at 50 Hz (Fig. 7*A*). While stimulation of the axon was continued, the membrane was slightly hyperpolarized (Fig. 7*B*). This resulted in an increase in the size of the decremental potential, but the increase did not reach threshold for spike initiation in the recording area. However, with stronger hyperpolarization (Fig. 7*C*) the decremental potential grew to reach threshold and it initiated a conducted spike, in spite of the continuous stimulation at 50 Hz. When the injection of the inward current was stopped (Fig. 7*D*), conduction was immediately blocked, and a decremental potential of even smaller amplitude than that seen originally was observed. The small size of the remaining decremental potential probably resulted from the continuously accumulating effect of stimulation at 50 Hz during the hyperpolarization period. We showed in Figs. 2*D* and 3 that the continuation of stimulation after the block had occurred causes a reduction in the size of the decremental potential.

The effects of membrane hyperpolarization on spike invasion at low stimulation frequencies strengthen the above finding. At low stimulation frequencies (Fig. 7*E–H*) hyperpolarization prevented the invasion of spikes into the recording area. It should be emphasized that such hyperpolarization is not sufficient to block conduction in the abdominal region. It seems that the hyperpolarization is effective in the ganglion T_3 region because this region has a special geometry (5, 35) and has a low safety factor for spike conduction.

Increase in membrane conductance

Another factor which probably contributes to conduction blocking is the increase in the axonal membrane conductance observed during and after high-frequency stimulation. Reduction in effective membrane resistance (Re) during high-frequency stimulation may be a direct result of the membrane depolarization since the giant axons membrane rectifies strongly in the depolarizing direction (4, 45). In this case the changes in Re should follow the membrane current-voltage curve. Namely, an identical depolarization produced by outward current injec-

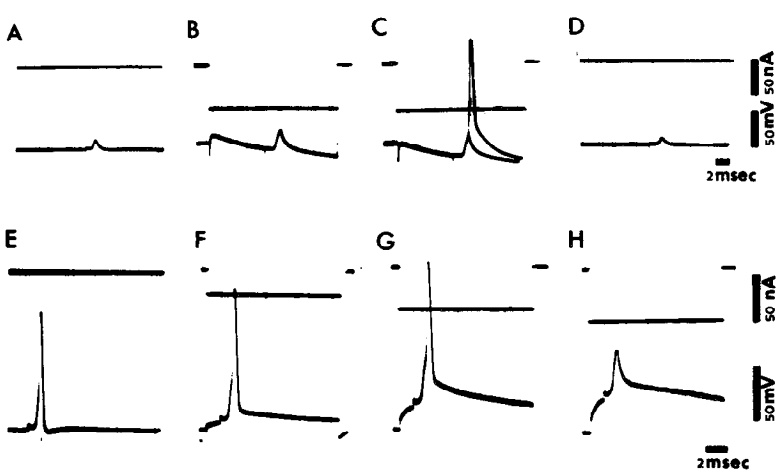

FIG. 7. *A–D*: effect of hyperpolarization on the frequency block, produced by continuous stimulation at 50 Hz. Upper trace monitors current injection. *A*: decremental potential of 9 mV after block had occurred; *B*: increase in the amplitude of the decremental potential to 18 mV as a result of hyperpolarization; *C*: after stronger hyperpolarization, the decremental potential grew in amplitude to reach spike threshold; *D*: after cessation of inward current injection, a decremental potential of only 4.5 mV was observed; *E–H*: effect of hyperpolarization on conduction of a single impulse; *F*: control; *F–H*: with growing hyperpolarization the invasion of the spike into the recording zone is blocked.

tion should give the same reduction in Re. Figure 8*A* shows that this is not the case.

The dependence of Re on membrane potential is given in Fig. 8*A* (filled circles); 8-mV depolarization produced about 75% reduction in Re. After stimulation of the whole connective at 100 Hz and the development of conduction block, the membrane was depolarized by about 18 mV and Re was reduced by about 90% (Fig. 8*A*, filled squares); 10 s later Re was 75% of the control (Fig. 8*A*, open squares). It is interesting to note that a few seconds later the membrane potential returned to the control level but Re was still reduced by about 50%. Only with a long period of rest (10 min) did Re return to the control level (Fig. 8*A*, open circles). These results show that the large decrease in Re observed after high-frequency stimulation of the whole connective results from a factor other than membrane depolarization. Such a factor can be the activation of synaptic inputs into the giant axons in ganglion T_3. Indeed it is shown in a later paragraph that the giant axons in ganglion T_3 do receive synaptic inputs. Moreover, these synapses are activated by stimulating the whole connective, and produce an increase in membrane conductance and conduction block. However, at this stage the presentation is limited to those results showing that conduction block can be achieved without the activation of these synapses and to support the hypothesis that under such conditions the main mechanism producing the conduction block is the increase in extracellular potassium concentration, causing membrane depolarization and sodium inactivation.

Can the conduction block be induced by stimulating a single axon?

It was found that intracellular stimulation of a single giant axon does not result in activation of discernible synaptic potentials in the same giant axon. Therefore, it was checked whether stimulation of a single giant axon can produce the conduction block and whether it is possible to account for the changes in Re by the membrane depolarization. It was found that the period of stimulation of a single axon required to lead to a conduction block was 6–10 times longer (at 50 Hz) than with stimulation of the whole connective. The change in Re, although not as pronounced as with whole connective

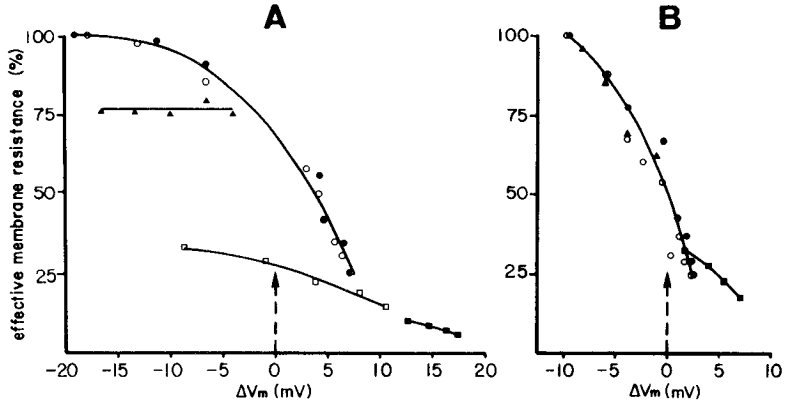

FIG. 8. Effective membrane resistance (Re) and its dependence on changes of membrane potential (ΔV_m). Re is given as a percent of its maximal value. Arrows indicate the effective membrane resistance at resting potentials, which in the graph are given as zero. Stimulation of a single giant axon (intracellularly) or the whole connective at T_2–T_3 was at 100 Hz for a duration sufficient to produce conduction blocks. *A*: resting potential of the axon was 77 mV and Re at that point in the control was 2 MΩ. Filled circles: control experiment, Re of a nonstimulated axon. Note the strong rectification. Filled triangles: Re, 1 s after stimulation of the single giant axon from which response was recorded. There was no depolarization but Re dropped by about 25%. Filled squares: 1 s after stimulation of the whole connective. The strong depolarization (18 mV) shifted the curve strongly to the right. Because of the shunting it was impossible to hyperpolarize the membrane beyond the point given. Open squares: 10 s later the membrane repolarized by about 8 mV and Re was still greatly reduced. Open circles: only after 10 min of rest did Re recover to the control curve. *B*: a similar experiment in a different axon in the same preparation but this time after preincubation for 30 min in *d*-TC 10^{-3} M. Resting potential was 72 mV and Re at rest was 1 MΩ. Filled circles: control. Re of a nonstimulated axon; note the rectification response. Triangles: after stimulation of the single axon. Re changes with membrane potential as in the control. Squares: 1 s after stimulation of the whole connective. The membrane depolarized by only 7 mV and shunting was not as large as before (compare *A* and *B*, filled squares). Also note that the curve still shows rectification. Open circles: after 40 s of rest, Re recovered to the control.

stimulation, was still larger than that expected from the membrane potential-Re dependence (Fig. 8*A*, filled triangles). But, in contrast with the result of whole connective stimulation, the recovery of Re to the control level was very fast, in the range of a few seconds. In order to find if the deviation of Re from the control curve resulted from synaptic activation (for example, increase in extracellular potassium could depolarize presynaptic terminals to increase spontaneous transmitter release (27)) the experiment was repeated in 10^{-3} *d*-TC, which was found to block these synaptic inputs. Under this condition, stimulation of a single axon at 100 Hz produced conduction block and the changes in Re could be accounted for by the membrane depolarization (Fig. 8*B*, filled circles and filled triangles). In the *d*-TC preparation stimulation of the whole connective produced a larger change in Re (Fig. 8*B*, filled squares) but not as large as in the control. The recovery of Re was rapid, in the range of a few seconds (Fig. 8*B*, open circles). The single-axon-stimulation experiment was also repeated in a preparation immersed in a free Ca-high magnesium (9 mM) solution. After testing that transmission across known synapses (e.g., cercal nerve-giant axon synapse and the T_3 inputs to the giant axons) was blocked, we found that conduction block could be obtained after stimulation at 50–100 Hz. We conclude that activation of synapses is not necessary in order to develop conduction block, although it can accelerate it.

Synaptic inputs on giant axons in ganglion T_3

After finding the large changes in membrane conductance seen after stimulation of the whole connective, we looked for synaptic inputs on the giant axons. A microelectrode was inserted into a giant axon as close as possible to the posterior base of ganglion T_3, and recordings were taken at high gain.

Synaptic potentials (PSP) were elicited by stimulation of the ipsi- or contralateral connectives at T_1–T_2, T_2–T_3, or at any level of the abdominal connectives. Figure 9 shows examples of synaptic potentials evoked at T_1–T_2. Stimulation at a low intensity, insufficient to stimulate the giant axons directly, induced 0.25–3 mV PSP with a latency of 8 ms or longer. Gradually increasing the stimulus intensity produced an increase in the amplitude of the PSPs in discrete steps, probably by the recruitment of new neuronal elements (Fig. 9*B–E*). These later PSPs could be evoked only by stimulation of the connectives anterior to ganglion T_3.

When the stimulus intensity was such that the giant axons were directly stimulated, a faster group of PSPs was seen. This suggests a synap-

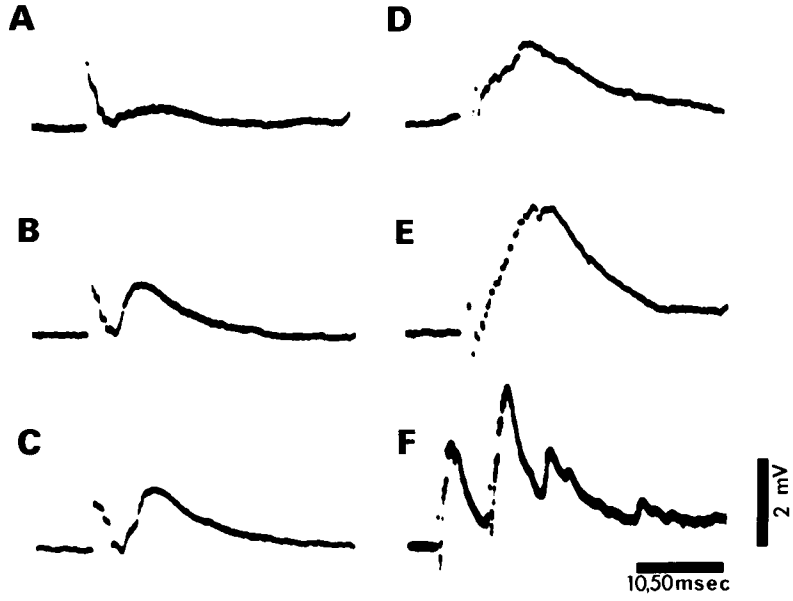

FIG. 9. Synaptic potentials recorded at the caudal base of ganglion T_3 to stimuli applied at T_1–T_2 ipsilateral connective. *A–E*: with gradual increase in stimulus intensity the amplitude of the PSP increased in discrete steps. Note the compound nature of the response. *F*: a twin response at a slower recording speed. Note the facilitation and the slower group of PSPs appearing on the right.

tic relationship among giant axons themselves. In order to test this possibility two microelectrodes were inserted into different giant axons. Activation of one giant axon induced a synaptic potential in the second axon, and vice versa (Fig. 10*A*, *B*). Synaptic connectivity, however, was not always found between the giant axons. In some cases, a synaptic response could be evoked only from one of a pair of giant axons. In other cases, no synaptic connectivity was seen at all. The synaptic potentials induced by giant axon stimulation are sensitive to high-frequency stimulation, and fatigue rapidly at 20 Hz. Stimulation of the cercal nerves also evoked PSPs in the giant axons (Fig. 10*C*). Thus, PSPs could be elicited by stimulation of neighboring giant axons, other elements within the ipsilateral and contralateral connectives, and from the cercal nerves. Synaptic potentials could not be seen in the giant axons after activation of the various nerve roots of ganglion T_3. At this stage, however, we cannot exclude the possibility that there exist other synaptic inputs not picked up by the electrode either because of their electrical remoteness or because their reversal potential is close to the resting potential.

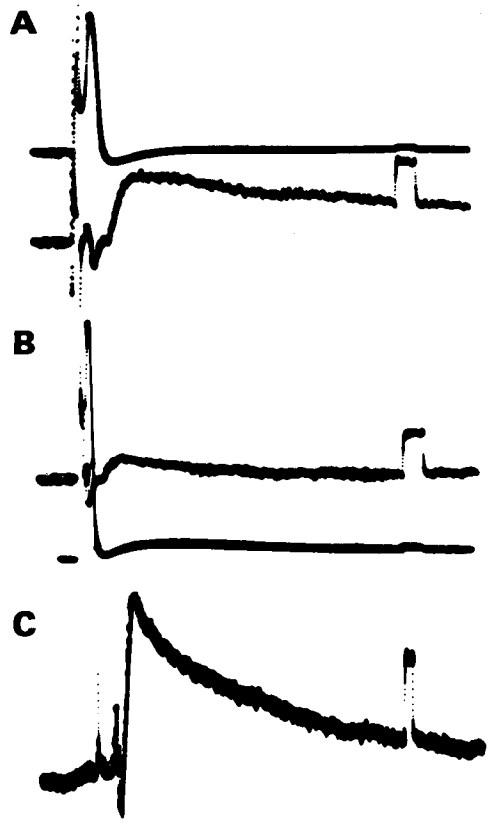

FIG. 10. Synaptic interactions between giant axons. Two giant axons were impaled with microelectrodes. The upper and lower sweeps are from electrodes in the anterior and posterior ends of ganglion T_3, respectively. *A*: stimulation of one axon (upper sweep) evoked a PSP in the second. *B*: stimulation of the second axon (lower sweep) evoked a PSP in the first. *C*: another preparation. Stimulation of the cercal nerves evoked PSPs in the giant axon at the caudal base of T_3. *A*, *B*: 1 mV, 1 ms. *C*: 1 mV, 2 ms.

The synaptic potentials described above are probably all mediated chemically as their amplitude was increased by hyperpolarization (Fig. 11*C*) and decreased by depolarization (Fig. 11*A*), and they were blocked either by *d*-TC (Fig. 11*D–F*) or by low Ca^{2+}-high Mg^{2+} (not shown). Unfortunately, it was not possible to determine the reversal potential of the PSPs directly because it was difficult to depolarize the membrane above the level where the delayed rectification became pronounced. As estimated by extrapolation, however, the reversal potential probably fell between −75 and −65 mV. This is very close to the threshold for spike initiation. Nevertheless, it was impossible to evoke a spike in the giant axon by synaptic activation at low- or high-stimulation frequency. Thus, we cannot determine from these data whether the synaptic potentials are excitatory or inhibitory in the classical sense.

Modulating effect of synaptic inputs on frequency block

The effects of the synaptic inputs on spike conduction in the giant axon was studied in the following way. The time required for development of a block by stimulation at 60 Hz of a single giant axon T_2–T_3 (50 s) was determined. After a long recovery period this experiment was repeated but this time, in addition to stimulation of the giant axon at T_2–T_3, synaptic inputs to it were activated by stimulation of the contralateral connective at T_1–T_2. Immediately, intermittent failures of axonal conduction at T_3 were observed and the latency for development of a conduction block became shortened from 50 s to only 7 s. On cessation of the activation of the contralateral synaptic inputs, conduction was restored. Finally, after a long recovery period, the giant axon was again stimulated at T_2–T_3 alone, and frequency block once more developed after about 50 s, as in the control experiment. In a *d*-TC-treated preparation, stimulation of the contralateral connective was ineffective in modulating giant axon conduction.

Other experiments demonstrating the modulatory effects of synaptic inputs on frequency blocking are given in Figs. 12–14. In Fig. 12 a

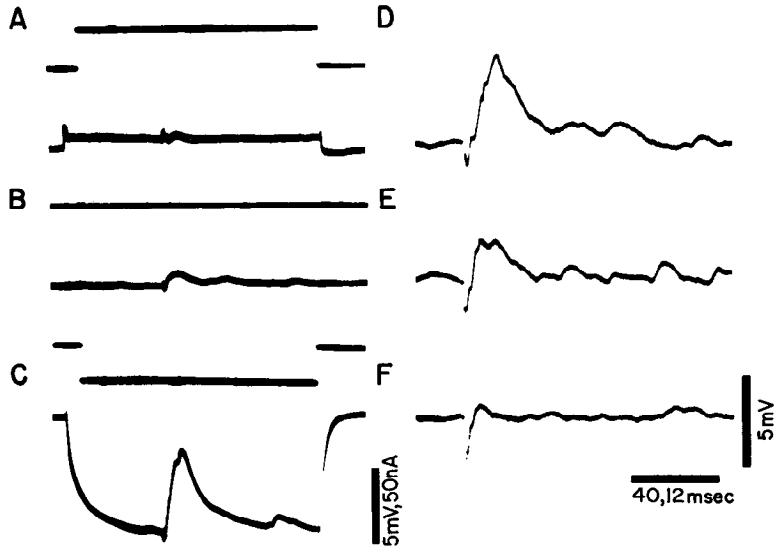

FIG. 11. Effect of depolarization (*A*) and hyperpolarization (*C*), on the amplitude of a PSP (*B*) evoked at T_1–T_2 and recorded at the posterior base of ganglion T_3. Current (upper sweep) was injected via a bridge circuit *A*–*C*, time scale 40 ms. *D*–*F*: effect of *d*-tubocurarine on synaptic potentials recorded at the posterior base of ganglion T_3 after stimulating the contralateral connective at T_2–T_3. *D*: control; *E*: after 7 min in 10^{-3} M *d*-Tc. *F*: after 15 min in *d*-Tc, the PSPs were blocked; *D*–*F*: time scale 12 ms.

train of 4 spikes separated by 4 ms was elicited by stimulation of the ipsilateral connective at a repetition rate of 3/s. At this repetition rate the 4 spikes were conducted faithfully for a long period (30 min, Fig. 12*A*). When a single impulse was delivered to the contralateral connective just before the fourth impulse of a train (Fig. 12*B*, arrow), however, the last spike of the train failed to invade the recording zone and only a decremental potential was observed. On

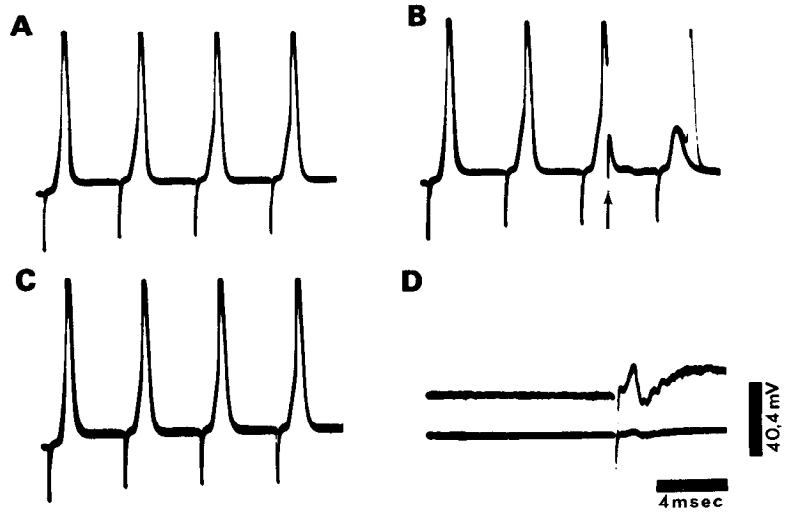

FIG. 12. Effect of the synaptic inputs on the pattern of a burst of spikes. *A*: control, 4 spikes separated by 4 ms were elicited by stimulation of the ipsilateral connective at T_2–T_3 and recorded at the caudal base of ganglion T_3. Repetition rate was 3 Hz. Responses presented in *A*–*C* are composed of three superpositions of sweeps. *B*: a synaptic potential was evoked by stimulation of the contralateral connective at T_1–T_2 and timed to arrive 2.5 ms before the fourth spike (arrow). Note that the fourth spike was blocked. *C*: immediate recovery after the removal of the synaptic activation. *D*: the synaptic potential alone at the same sweep speed as in *B* to show its relation to the fourth spike. Calibration of upper sweep in *D*: 4 mV, 4 ms.

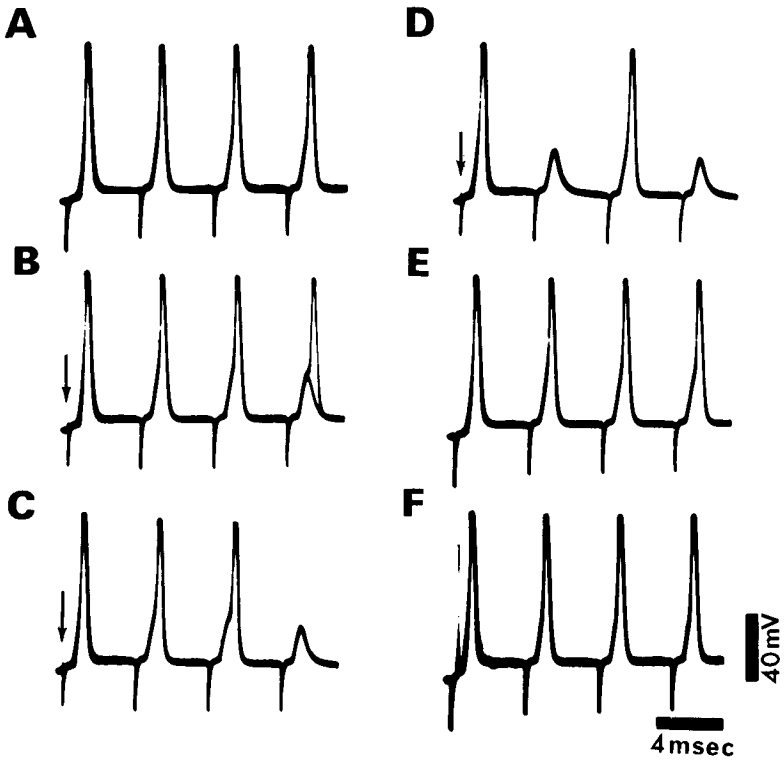

FIG. 13. Same experiment as in Fig. 12, but the stimulation to the contralateral connective to elicit the synaptic input precedes the first spike in the burst by 1.1 ms (arrows). *A*: control; *B*: 1 s after the synaptic input was activated, the fourth spike was blocked. *C–D*: 2 and 5 s later. *E*: 10 min after the removal of the synaptic input the burst recovered. Between *E* and *F* the synapse was fatigued by stimulation at 100 Hz for 2 min. *F*: same conditions as in *B*, but now the synaptic potential had no effect on the burst.

removal of this synaptic input, conduction again returned to normal (Fig. 12*C*). Again *d*-TC treatment canceled the contralateral synaptic effect.

In the experiment shown in Fig. 13 we demonstrate that the modulation capacity of the synaptic inputs on spike trains varies with time. When single impulses were delivered to the T_1–T_2 contralateral connectives, timed to precede each train by 1.1 ms, the effect of this synaptic input on conduction of the 4 spikes varied with time and different spikes in the train were blocked (Fig. 13*C*, *D*). On cessation of the synaptic input, the 4 spikes reappeared. At this stage the giant axon was given a rest and the synaptic input was fatigued by stimulating the T_2–T_3 connectives at 100 Hz for 2 min (a period long enough to outlast lingering effects of the synapses at this frequency, see next paragraph). After this period, in which the contralateral connective was continuously stimulated, the effectiveness of synaptic modulation on conduction of the 4 spikes was again tested as before. Now the synaptic input was ineffective and did not block conduction of any of the spikes (Fig. 13*F*).

The experiment illustrated in Fig. 14 shows that synaptic inputs elicited by stimulation of the contralateral connective alone (without simultaneous activation of the giant axons) is sufficient to produce conduction block. The contralateral connective at T_1–T_2 was stimulated at 20 Hz for 30 s (not shown). Then, stimulation of the synaptic input was stopped and the giant axon was stimulated again with trains of spikes as before. Figure 14*B* shows that immediately after cessation of the synaptic activation the four impulses were blocked. By 20 s later (Fig. 14*C*), the first spike in the train had recovered. After 40 s (Fig. 14*D*), the third spike also recovered. After 45 s, only the third spike remained blocked (Fig. 14*E*). It required 50 s before complete recovery of all four impulses was observed. From these results we conclude that *a*) activation of the synapses alone is sufficient to produce conduction block

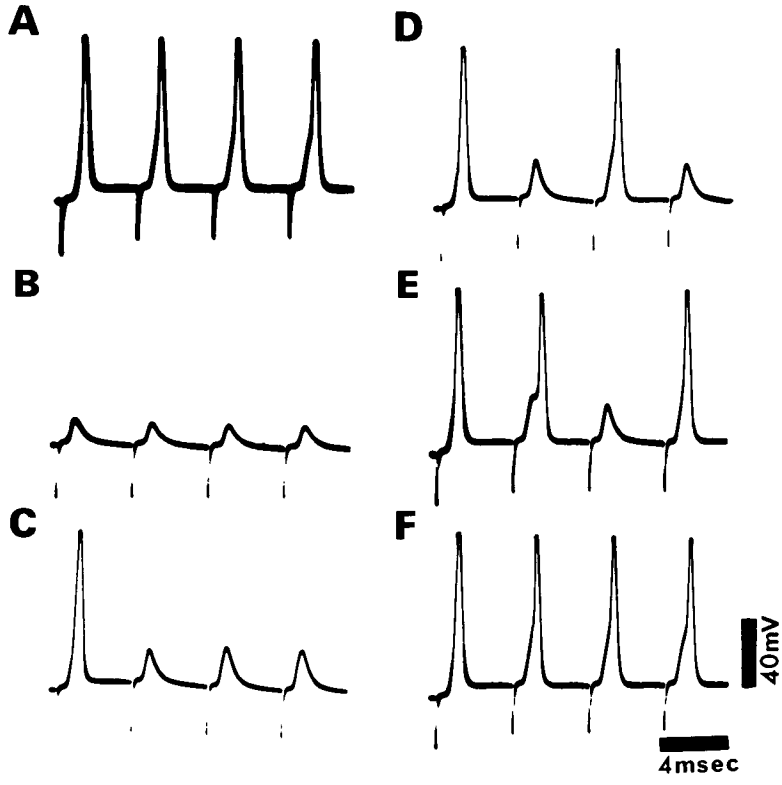

FIG. 14. Lingering effects of the synaptic inputs. Same experiment as in Figs. 12 and 13. *A*: control. Between *A* and *B* the synapses were activated alone at 20 Hz for 1 min. *B*: 1 s after cessation of the synaptic activation. The T_2–T_3 ipsilateral connective was stimulated as before. Note that all 4 spikes are still blocked. *C*: after 20 s only the first spike recovered. *D*: after 40 s; *E*: after 45 s; *F*: after 50 s there was a recovery of the burst.

along the giant axons in ganglion T_3, and *b*) the effects of the synaptic inputs outlast their stimulation period by many seconds.

DISCUSSION

The present results demonstrate that axons in regions of special geometry have the capacity to change the pattern of impulses that propagate along them, a property classically assigned to chemical synapses. The finding of synaptic inputs on the giant axons in ganglion T_3 changes this system from a relatively simple model to a much more complicated one. Nevertheless, the relative contribution of these synaptic inputs on the conduction block could be eliminated either by the use of *d*-TC or by free Ca^{2+}-high Mg^{2+} solutions. Thus it was possible to isolate the nonsynaptic effects at high frequency of stimulation, effects which we would like to discuss first.

Our electrophysiological observations suggest that a gradual reduction in safety factor for impulse propagation occurs along the second and third quarters of ganglion T_3. This conclusion is based on the findings that decremental potentials of a similar amplitude could be recorded both at the anterior and posterior ends of ganglion T_3 after the frequency block had developed. Morphological studies show that in this same region the giant axon narrows and sends off several branches which ramify to form a tree (5, 10, 13, 31, 35). In the present paper and these that follow (5, 26), we wish to argue that the special geometry of the axon is the cause of the low safety factor for impulse propagation at this region. It is clear that at low stimulation frequencies the safety factor for spike propagation is sufficient to allow a 1:1 transmission. On repetitive activation of the giant axon itself or together with its neighboring axons, however, a gradual reduction of the safety factor at the regions of block takes place.

These findings call for an extension of Rall's (32) computations for impedance matching at branching points. His computations are rele-

vant to nonexcitable membrane such as that of many dendrites or, at most, for the propagation of a single impulse without long-lasting changes in membrane resistance. Such a theoretical analysis must take into account dynamic changes which occur during repetitive activation of the axon, and this is the topic of a later paper in this series (26).

In the present paper we have examined the dynamic changes that lead to the lowering of the safety factor and to a conduction block at high frequencies.

Membrane depolarization

The development of conduction block is associated with membrane depolarization and a decrease of the afterhyperpolarization. Similar changes in membrane potential after activation at high frequency were seen by Frankenheuser and Hodgkin (11) in the isolated squid giant axon. Such depolarization was shown to be produced by an increase of the extracellular potassium concentration. Pichon (30) showed that the cockroach giant axons behave very much like the squid giant axon. Baylor and Nicholls (2), using the leech glial cell as a potassium electrode, showed that high-frequency stimulation of neighboring cells increase extracellular potassium concentration. Frankenheuser and Hodgkin (11) calculated that the increase in extracellular potassium concentration after one impulse can reach values of 1 mM, and in closely packed axons 4 mM, per impulse (9).

The membrane depolarization seen in the cockroach giant axon varied with the frequency of stimulation and reached values as high as 18 mV at 100 Hz. Computed from the Nernst equation, such depolarization corresponds to an increase of 3.4 mM in extracellular potassium at the point of recording.

We found no clear correlation between the rate of the development of the depolarization, its maximal level, and the time required to develop a block at different frequencies of stimulation. It seems that at relatively low frequencies (30–40 Hz) additional mechanisms, such as synaptic inputs, contribute to the development of the frequency block. At high frequencies (60–100 Hz), the membrane depolarization is large and is sufficient to explain the development of the block. Injection of outward current pulses of 2–3 s to produce similar depolarizations also caused a conduction block.

Changes in afterhyperpolarization

One of the parameters that Frankenheuser and Hodgkin (11) used to indicate changes in extracellular potassium ions was the size of the afterhyperpolarization. During the period of the hyperpolarization the membrane potassium conductance is high also in the cockroach (30), and many workers use the hyperpolarization as indicating the potassium equilibrium potential (2, 3, 11, 22).

The change in the size of the afterhyperpolarization seen, for example, after stimulation at 50 Hz, was 3.8 mV, indicating an increase in extracellular potassium concentration of 4 mM, a value which corresponds well with the value computed from the change in membrane potential and which strengthens the hypothesis that the membrane depolarization is mainly produced by extracellular potassium accumulation. Activation of the synaptic inputs (whole connective stimulation) did not produce much larger depolarization. This can be explained by the finding that the synaptic reversal potential is around −65 to −75 mV. On the other hand, the synapses had a marked effect on membrane conductance.

Reduction of effective membrane resistance

During and after stimulation at high frequency and concomitantly with the membrane depolarization, the effective membrane resistance (Re) of the fiber fell markedly. The reduction of Re may have been the result of either delayed rectification and/or an increase in membrane conductance produced by activation of synaptic inputs to the giant axon in ganglion T_3.

Though it is clear that the membrane depolarization during and following high frequency activation contributes to the drop in Re (delayed rectification), the amount of depolarization was insufficient to account for all of the observed drop in Re. Furthermore, the time to a complete recovery of the membrane potential was much shorter than that for the recovery of Re. This finding indicates that other mechanisms than the localized and direct membrane depolarization are involved in the drop of Re.

A possible mechanism to account for the large and long-lasting drop in Re is the activation of synaptic inputs by stimulation of the connectives at high frequency. It is clear, however, that under experimental conditions where only one giant axon is activated or where all apparent synaptic activity is blocked either by high Mg^{2+} with low Ca^{2+} or by *d*-tubocurarine, stimulation of the giant axon at high frequency still produces the high-frequency block, and now the changes in conductance could be ac-

counted for by the delayed rectification. This shows that in order to produce the block, activation of chemical synapses at this region is not essential.

Changes in size of action potential

The changes observed in the size of the action potential could be explained by partial sodium inactivation produced by the membrane depolarization (15, 30). In addition, the increase in extracellular potassium concentration by itself would facilitate sodium inactivation (1). Finally, it is possible that the increase in intracellular sodium concentration, which occurs during the high-frequency activation of the fiber, lowers the driving force for sodium currents.

These factors, however, are insufficient to explain the development of conduction block at T_3. Similar changes which probably occur along the abdominal portion of giant axon do not lead to a conduction block. In previous studies (28) it was shown that conduction block at high-frequency stimulation occurs only at T_1, T_2, and T_3. The relatively large increase in load resistance imposed by the giant axon branches and the increase in axon diameter in front of the propagating action-potential wave, reduce the spike amplitude before the point of enlarged surface area (7, 12, 21, 33). As the local resistance decreases, more current is shunted until the action potential before the point of the low safety factor at the giant axon is too small to depolarize it above threshold.

Conduction block of impulses has by now been demonstrated in several preparations (6, 12, 14, 23, 41, 43). One common characteristic in all these cases is that the axons have a zone with a special geometry, such as a bifurcation or a step with an increased diameter. The second common feature is that the "filtering capacity" (conduction block) appears following stimulation at high frequency. Although the sequence of events leading to the conduction block is similar in the different preparations, the mechanisms involved are different. In the sensory neurons of the leech, conduction block and differential channeling of action potentials are due to membrane hyperpolarization resulting from the activation of an electrogenic pump (17, 41). In this case the conduction block could be relieved by application of strophanthidin. In the common axon innervating the deep abdominal extensor muscles of the crayfish and lobster (23), conduction block is apparently associated with an increase of the membrane threshold for spike initiation due to partial sodium inactivation. This inactivation is associated with only a small membrane depolarization (25). In the giant axon of the cockroach it seems that the dominant factor leading to the frequency block is the shunting of current by the large increase of the membrane conductance at the narrower section of the axon in ganglion T_3 and its branches.

Synaptic inputs

The giant axons of the cockroach differ from other experimental models (12, 14, 41) by the finding of synaptic inputs on them. Ultrastructural data are now available to support the presence of synaptic inputs on branches of the giant axons in ganglion T_3 (5). Because of the special geometry of the axon, the synaptic inputs are effective in modulating spike propagation across ganglion T_3 in both the ascending and descending direction.

Under our experimental conditions the presynaptic elements were not able to evoke an action potential in the giant axon. Since it was not possible to determine accurately the reversal potential of the synapses, we do not know whether it is above or below the threshold for spike initiation. It is, therefore, impossible to determine whether the synapses are excitatory or inhibitory in the classical sense. Modulation of spike trains is apparently produced by increasing the membrane conductance and shunting of current in a region of a low safety factor. A somewhat similar situation is found in dendrites where activation of proximal synapses reduces the space constant for decremental conduction and, therefore, the effectiveness of distal synaptic inputs (16).

Another possible role for the synapses situated on the branches of the giant axons is that they serve as presynaptic inhibitors of information going out from the giant axons to neurons in ganglion T_3. Such giant axon outputs have already been demonstrated both electrophysiologically (ref 8 and Fig. 10) and structurally (5).

The finding of synaptic inputs on the giant axons and the demonstration that they can modulate the reliability of conduction suggests an explanation to some of the findings in the experiments where the whole connective was stimulated. In these experiments it was shown that the time required to develop a frequency block is much shorter in comparison to that observed when a single axon is stimulated. One possible explanation is the more rapid buildup of extracellular potassium concentration caused by the stimulation of neighboring axons (9). In the context of the present work it is clear that stimulation of the whole connective involves also the activation of synapses which produce a large increase in membrane conductance. This change in membrane conductance would be ex-

pected to decrease the time required to develop a conduction block.

It is difficult to determine the relative contribution of synapses to the increase in membrane conductance. Even when a single axon was stimulated, membrane conductance was increased more than expected from rectification alone, although the difference was less than after stimulation of the whole connective. The finding that giant axon collaterals synapse on other neurons makes it possible that even under conditions of single axon stimulation, synaptic inputs to the same axon may be activated either directly or through interneurons. Such synaptic activation, however, is not necessary to bring about a frequency block as was shown by the *d*-TC experiments and also predicted theoretically (26). Another possible mechanism is that potassium accumulating around the axon depolarizes neighboring terminals which, in turn, release greater amounts of transmitter substance. Such effects of transmitter released tonically on membrane conductance have been demonstrated recently (27). The finding that the time required for recovery of the membrane conductance after stimulation of a single giant axon is very short and, indeed, similar to the time required for the membrane to repolarize, supports the later mechanism. It was also shown that after frequency block by high-frequency stimulation of the whole connective had been established and the stimulation stopped, the giant axon membrane conductance remained high for at least a few minutes in spite of the rapid repolarization of the membrane potential (complete repolarization within a few seconds). The lingering effect of synaptic inputs after cessation of stimulation offers a possible explanation. That is, the long-lasting effect of the synapse could maintain an increased membrane conductance without necessarily being associated with a prolonged local membrane depolarization either because of nearness of the PSPs reversal potential to that of the resting potential or because of the electrical distance of the synaptic input. The mechanisms involved in the long-lasting effects of the synapses are not clear. The effect could, however, result either from a prolonged synaptic action similar to that described for inhibition of long duration (19, 24, 29, 39) or to a repeated activation of the synapses through reverberatory circuit. The ultrastructural study of Castel et al. (5) showing reciprocal synaptic foci in the giant axons in ganglion T_3 makes the later assumption workable even without the actual propagation of action potentials.

The special architecture of the giant axons at the level of the T_3 ganglion, together with the synaptic inputs described, provide a fine mechanism for the control of frequency and patterns of giant axon spikes traversing ganglion T_3.

ACKNOWLEDGMENTS

We are grateful to Dr. M. Davor and Prof. P. Hillman for a critical reading of the manuscript. We are also grateful to Miss Ada Dorman for technical assistance in preparing the drawings.

This study was supported by Grant AS: 11 1955 from Stiftung Volkswagenwerk.

REFERENCES

1. ADELMAN, W. J. AND PALTI, Y. The influence of external potassium on the inactivation of sodium current in the giant axon of the squid. *J. Gen. Physiol.* 53: 685–703, 1969.
2. BAYLOR, D. A. AND NICHOLLS, J. G. Changes in the extracellular potassium concentration produced by neuronal activity in the central nervous system of the leech. *J. Physiol., London* 203: 555–569, 1969.
3. BRODWICK, M. S. AND JUNGE, D. Post stimulus hyperpolarization and slow potassium conductance increase in Aplysia giant neurone. *J. Physiol., London* 223: 549–570, 1972.
4. CALLEC, J. J. Etude de la transmission synaptique dans le system nerveux central d'un insecte (*Periplaneta americana*) (Ph.D. Thesis). Rennes, France: Universite de Rennes, 1972.
5. CASTEL, M., SPIRA, M. E., PARNAS, I., AND YAROM, Y. Ultrastructure of region of a low safety factor in inhomogenous giant axon of the cockroach. *J. Neurophysiol.* 39: 900–908, 1976.
6. CHUNG, S., RAYMOND, S. A., AND LETTVIN, J. Y. Multiple meaning in single visual units. *Brain Behav. Evol.* 3: 72–101, 1970.
7. COOMBS, J. S., CURTIS, D. R., AND ECCLES, J. C. The interpretation of spike potentials of motoneurons. *J. Physiol., London* 139: 198–231, 1957.
8. DAGAN, D. AND PARNAS, I. Giant fiber and small fiber pathways involved in the evasive response of the cockroach *Periplaneta americana*. *J. Exptl. Biol.* 52: 313–324, 1970.
9. ECCLES, J. C., KORN, H., TÁBOŘÍKOVÁ, H., AND TSUKAHARA, N. Slow potential fields generated in cerebellar cortex by mossy fiber volleys. *Brain Res.* 15: 276–280, 1969.
10. FARLEY, R. D. AND MILBURN, N. S. Structure and function of the giant fiber system in the cockroach *Periplaneta americana*. *J. Insect Physiol.* 15: 457–476, 1969.
11. FRANKENHEUSER, B. AND HODGKIN, A. L. The after effects of impulses in the giant nerve fiber of Loligo. *J. Physiol., London* 131: 341–376, 1956.
12. GROSSMAN, Y., SPIRA, M. E., AND PARNAS, I.

Differential flow of information into branches of a single axon. *Brain Res.* 64: 379–386, 1973.
13. HARRIS, C. L. AND SMYTH, T. Structural details of cockroach giant axons revealed by injected dye. *Comp. Biochem.* 40: 295–303, 1971.
14. HATT, H. AND SMITH, D. O. Axon conduction block: differential channeling of nerve impulses in the crayfish. *Brain Res.* 87: 85–88, 1975.
15. HODGKIN, A. L. AND HUXLEY, A. F. A quantitative description of membrane current and its application to conduction and excitation in nerve. *J. Physiol., London* 117: 500–544, 1952.
16. HUBBARD, J. I., LLINÁS, R., AND QUASTEL, D. M. J. In: *Electrophysiological Analysis of Synaptic Transmission.* London: Camelot, p. 212–257, 1972.
17. JANSEN, J. K. S. AND NICHOLLS, J. G. Conductance changes, an electrogenic pump and the hyperpolarization of leech neurones following impulses. *J. Physiol., London* 229: 635–655, 1973.
18. KENNEDY, D. AND MELLON, D. Synaptic activation and receptive fields in crayfish interneurons. *Comp. Biochem. Physiol.* 13: 275–300, 1964.
19. KEØHOE, J. Ionic mechanism of two-component cholinergic inhibition in *Aplysia* neurones. *J. Physiol., London* 225: 85–114, 1972.
20. KERKUT, G. A., PITMAN, R. M., AND WALKER, R. J. Iontophoratic application of acetylcholine and GABA into insect central neurons. *Comp. Biochem. Physiol.* 31: 611–633, 1969.
21. KHODOROV, B. I., TIMIN, Y. N., VILENKINS, S. Y., AND GULKO, F. B. Theoretical analysis of the mechanisms of conduction of nerve pulse over an inhomogenous axon: conduction through a portion with increased diameter. *Biofizika* 14: 304–315, 1969.
22. KUFFLER, S. W. Neuroglial cells: physiological properties and a potassium mediated effect of neuronal activity on the glial membrane potential. *Proc. Roy. Soc., London, Ser. B* 168: 1–21, 1976.
23. PARNAS, I. Differential block at high frequency of branches of a single axon innervating two muscles. *J. Neurophysiol.* 35: 903–914, 1972.
24. PARNAS, I., ARMSTRONG, D., AND STRUMWASSER, F. Prolonged excitatory and inhibitory synaptic modulation of a bursting pacemaker neuron. *J. Neurophysiol.* 37: 594–608, 1974.
25. PARNAS, I., GROSSMAN, Y., AND SPIRA, M. E. Changes in conductance and membrane potential associated with differential channeling of information in a bifurcating axon. *Israel J. Med. Sci.* 8: 106, 1975.
26. PARNAS, I., HOCHSTEIN, S., AND PARNAS, H. Theoretical analysis of parameters leading to frequency modulation along an inhomogeneous axon. *J. Neurophysiol.* 39: 909–923, 1976.
27. PARNAS, I., RAHAMIMOFF, R., AND SARNE, Y. Tonic release of inhibitory transmitter in the neuromuscular junction of the crab. *J. Physiol., London* 250: 275–286, 1975.
28. PARNAS, I., SPIRA, M. E., WERMAN, R., AND BERGMAN, F. Nonhomogeneous conduction in giant axons of the nerve cord of *Periplaneta americana*. *J. Exptl. Biol.* 50: 635–649, 1969.
29. PARNAS, I. AND STRUMWASSER, F. Mechanisms of long-lasting inhibition of a bursting pacemaker neuron. *J. Neurophysiol.* 37: 609–620, 1974.
30. PICHON, Y. Aspects electriques et ioniques du fonctionnement nerveux chez les insectes. Cas particulier de la chaine nerveuse abdominale d'une blatte *Periplaneta americana* (Ph.D. Thesis): Rennes, France: Universite de Rennes, 1969.
31. PITMAN, R., TWEEDLE, C. D., AND COHEN, M. J. The form of nerve cells determination by cobalt impregnation. In: *Intracellular Staining in Neurobiology,* edited by B. S. Kenter and C. Nicholson. New York: Springer, 1973, p. 83–97.
32. RALL, W. Theoretical significance of dendritic trees for neuronal input-output relations. In: *Neuronal Theory and Modeling,* edited by R. F. Reiss. Palo Alto, Calif.: Stanford Univ. Press, 1964, p. 73–97.
33. RAMON, F., JOGNER, R. W., AND MOORE, J. W. Propagation of action potentials in inhomogeneous axon regions. *Federation Proc.* 34: 1357–1363, 1975.
34. ROEDER, K. D. Organization of the ascending giant fiber system in the cockroach *Periplaneta americana*. *J. Exptl. Zool.* 108: 243–262, 1948.
35. SPIRA, M. E., CASTEL, M., AND PARNAS, I. Fine structure of the giant axons in the metathoracic ganglion of the cockroach, the low safety factor zone for spike propagation. *Israel J. Med. Sci.* 10: 5, 1974.
36. SPIRA, M. E., PARNAS, I., AND BERGMAN, F. Organization of the giant axons of the cockroach *Periplaneta americana*. *J. Exptl. Biol.* 50: 615–627, 1969.
37. SPIRA, M. E., PARNAS, I., AND BERGMAN, F. Histological and electrophysiological studies on the giant axons of the cockroach *Periplaneta americana*. *J. Exptl. Biol.* 50: 629–634, 1969.
38. SPIRA, M. E., PARNAS, I., YAROM, Y., AND GROSSMAN, Y. Long term changes in spike propagation in rumifying axons. *Intern. Congr. Physiol. Sci., 26th, New Delhi, 1974. Jerusalem Satellite Symp. Mechanisms of Synaptic Action 1974,* p. 56.
39. TAUC, L. Some aspects of postsynaptic inhibition in *Aplysia*. In: *Structure and Function of Neuronal Inhibitory Mechanisms,* edited by C. Von Euler, S. Skoglund, and U. Soderberg. Oxford: Pergamon, 1968, p. 377–382.
40. TAUC, L. AND HUGHS, G. M. Modes of initiation and propagation of spikes in the branching axon of the molluscan central neurons. *J. Gen. Physiol.* 46: 533–549, 1963.
41. VAN ESSEN, D. C. The contribution of membrane hyperpolarization to adaptation and conduction block in sensory neurons of the leech. *J. Physiol., London* 230: 509–534, 1973.
42. WATANABE, A. AND TAKEDA, K. The spread of excitation among neurons in the heart ganglion of the stomatopod *squilla* oratoria. *J. Gen. Physiol.* 46: 773–801, 1963.
43. WAXMAN, S. G. Regional differentiation of the

axon: a review with reference to the concept of the multiplex neuron. *Brain Res.* 47: 269–280, 1972.

44. WAXMAN, S. G., PAPPAS, G. D., AND BENNETT, M. V. L. Morphological correlates of functional differentiation of nodes of ranvier along single fibers in the neurogenic electric organ of the knifefish. *J. Cell Biol.* 53: 210–229, 1972.

45. YAMASAKI, T. AND NARAHASHI, T. Electrical properties of cockroach giant axons. *J. Insect Physiol.* 3: 230–242, 1959.